


Article

Deterministic vs. Random Modulated Interference on G3 Power Line Communication

Waseem El Sayed ^{1,2,*} , Piotr Lezynski ¹ , Robert Smolenski ¹ , Amr Madi ^{1,2} , Marcin Pazera ³ 
and Adam Kempinski ¹ 

¹ Institute of Automatics, Electronics and Electrical Engineering, The University of Zielona Gora, 65-417 Zielona Gora, Poland; p.lezynski@iee.uz.zgora.pl (P.L.); r.smolenski@iee.uz.zgora.pl (R.S.); Amr.madi@ieee.org (A.M.); a.kempinski@iee.uz.zgora.pl (A.K.)

² Marine Engineering Technology Department, College of Maritime Transport and Technology, Arab Academy for Science and Technology and Maritime Transport, P.O. Box 1029, Abou Keer Campus, Alexandria 21500, Egypt

³ Institute of Control and Computation Engineering, The University of Zielona Gora, 65-417 Zielona Gora, Poland; m.pazera@issi.uz.zgora.pl

* Correspondence: waseem.elsayed@ieee.org

Abstract: Power line communication (PLC), which is often used in advanced metering infrastructure (AMI), may be disturbed by adjacent high-power converters. Due to the inherent features of this type of communication, classic methods of improving communication reliability (filtration and circuit separation) cannot be fully applied. Information coding (modulation) methods are used in PLC to increase the data transfer rate and improve noise immunity. Random modulations (RanM) are used in converters to lower emission levels. Therefore, we investigate how the converters' modulation parameters and coding methods may affect PLC communication reliability in the paper. To this end, we employ an experimental approach. In particular, the analysis of the influence of deterministic modulation (DetM) and (RanM) on the performance of narrowband G3-PLC is shown. We emulated an actual situation where EMI generated by the DC/DC converter disturbed the PLC transmission. The experimental results show the transmission error rates for different operating scenarios. The natural (experimental) system results, due to the complexity of the disturbing signals, differ from the literature data obtained by simulation for normalized signals.

Keywords: power line communication (PLC); electromagnetic interference (EMI); random modulation



Citation: Sayed, W.E.; Lezynski, P.; Smolenski, R.; Madi, A.; Pazera, M.; Kempinski, A. Deterministic vs. Random Modulated Interference on G3 Power Line Communication. *Energies* **2021**, *14*, 3257. <https://doi.org/10.3390/en14113257>

Academic Editor: Acha-Daza Enrique

Received: 15 April 2021

Accepted: 31 May 2021

Published: 2 June 2021

Publisher's Note: MDPI stays neutral with regard to jurisdictional claims in published maps and institutional affiliations.



Copyright: © 2021 by the authors. Licensee MDPI, Basel, Switzerland. This article is an open access article distributed under the terms and conditions of the Creative Commons Attribution (CC BY) license (<https://creativecommons.org/licenses/by/4.0/>).

1. Introduction

Power line communication (PLC) may be used in the smart grid, e.g., in metering systems [1] and industrial systems [2]. The PLC uses the existing power cables for data transmission, which leads to reduced investment and maintenance costs. However, many problems can appear, especially in the PLC that works in the frequency band between 2–150 kHz. Typically, the source of the problem is the high-level of electromagnetic interference (EMI). These EMI in the power grid are generated by energy receivers (electric drives, lighting, household appliances, and computers) [3] and renewable energy sources [4,5]. In both cases (energy consumption or generation), the sources of EMI are power electronics circuits. The main reason is the fact that power electronics utilize a switching frequency that may overlap with the PLC working frequency range [6,7]. Since the communication signals and disturbances generated by power electronic converters occur in the same frequency band, bandpass filters installed in communication devices cannot provide specific protection. Thus, if the amplitude of a disturbance approaches a high enough level, communication errors occur [8]. The signal to noise ratio factor (SNR) usage is a common approach to the fast evaluation of transmission and its channel quality. However, the shape and nature of the interference signals that do not affect SNR directly are also crucial for their impact on communication error rates.

In [9,10], the authors divided the PLC disturbing signals into four types: background noise, narrowband noise, periodic impulsive noise, and asynchronous noise. Communication engineers typically test data transmission systems (also PLC) using standardized disturbing signals (white noise, periodic impulse noise, and narrowband noise). Information encoding methods are tested, e.g., BPSK, QPSK, and 8PSK, to improve data transfer rates and immunity to disturbances [11]. However, the real signals are more complicated and are a composite of these basic types [12]. Therefore, many researchers choose an experimental approach by studying the impact of real sources (power electronic converters) on the operation of existing communication systems, specifically with the conventional deterministic modulation (DetM) [13–15]. In [13], where the communication data transmission errors in the RS232 communication protocol were addressed based on the effect of the power converter modulation, the study presents a mathematical model for estimating the percentage of data transmission errors relative to the switching frequency. In [15], the study addressed the influence of power converter cables in the induction motor drive system on RS485 communication. The effect of the periodical pulse generated by a pulse generator on the RS232 and RS485 using the mutual coupling between cables was addressed in [14].

On the other hand, many studies have been conducted on the application of the randomized PWM (RanM) techniques for EMI mitigation. Those randomized techniques spread the power of the signal into a broad band of frequencies and change the shape of the interference spectrum [16–18]. As a result, the level of the spectrum is significantly reduced. From the EMC point of view, utilization of a RanM is the right approach to reducing the EMI level below limits described in EMC standards [19]. However, low numbers of studies have been conducted to check the practical effect of the RanM on telecommunication devices [20,21]. Some studies confirm no difference between the DetM and RanM, especially in the uncoded communication systems, where the observed statistics of communication error are comparable or inconclusive [13,21]. It has also been shown that the reduction of the EMI level provided by randomly modulated converters results from the methodology of measurement. Changing the settings of the EMI receiver, one may significantly change the level of the measured disturbances for pseudo-randomly modulated converters [18]. The authors overviewed existing spread spectrum techniques and evaluated these techniques in the class-D converter. Moreover, the authors noted the impact of spectrum measurement on the results and the choice of spread spectrum modulation. Other studies confirm that the total power/energy of disturbances for RandM is the same as in DetM. By selecting the appropriate measurement parameters and spectrum aggregation, the exact measurements are obtained for RanM and DetM [22,23].

Considering state-of-the-art literature, the probability of data transmission error resulting from the interference between the power electronic device and the PLC is one of the critical factors conditioning reliable operation of a smart grid consisting of power electronic interfaces and PLC-based AMI. The purpose of this paper is to answer an essential question, i.e., what is the difference between the influence of the standard DetM and the RanM on the transmission reliability of narrowband G3-PLC? In the paper, a comparison between the influence of DetM and RanM on the frame error rate in the G3-PLC system has been shown to an extent not previously presented in the literature. The article's main contribution is to show the differences between DetM and RanM regarding the impact on PLC communication systems that use advanced data encoding methods and input selectivity. In addition, the article investigated the influence of data encoding methods on the immunity to disturbances. The results may be surprising as the data are known from the literature so far are slightly different.

2. Random Modulation vs. Deterministic Modulation

Pulse width modulation (PWM) is commonly used to control a DC/DC converters. In the DetM strategy, the PWM signal is generated by comparing the reference value (related to a converters output voltage) with a carrier signal of fixed frequency. Three main parameters can define the PWM signal: the period of the signal T (related to the

signal frequency f), the amplitude A , and the turn ON time of the signal α . The period T remains constant with the time, as shown in Figure 1a. In the frequency domain, spectral lines occur at fixed frequencies related to the carrier frequency and multiples, as shown in Figure 1c. For RanM, some of the signal parameters change randomly, such as the switching frequency or the duty cycle. In the RanM considered in the article, the carrier frequency f_n varies for every n th impulse (2) according to a driving signal R_n . The R_n could be sinusoidal function, triangle function, or randomized pulse amplitude modulated (PAM) function. Such RanM is called random carrier frequency Modulation with fixed duty cycle (RCFMFD). In this case, the period of the signal changes randomly, but the duty cycle remains constant with time, as shown in Figure 1b. The frequency and the duty cycle of the signal follow these equations:

$$f_n = f_{PWM} + \Delta f \cdot R_n, \quad R_n \in \langle -0.5 : 0.5 \rangle \quad (1)$$

$$\Delta f = f_{PWM} \cdot \beta, \quad \beta \in \langle 0.1 : 1 \rangle \quad (2)$$

where f_{PWM} is the fundamental frequency of the randomized signal. β represents the spreading factor of the RanM signal, and R_n represents a uniform distribution of pseudo-random numbers generated between -0.5 and 0.5 . This control approach provides the ability of spectrum shaping according to the standard requirements. Other types of RanM techniques are also investigated in literature [24,25]. In this paper, we utilize the RCFMFD as RanM technique for DC/DC converter due to the greatest impact on lowering the levels of interferences [23].

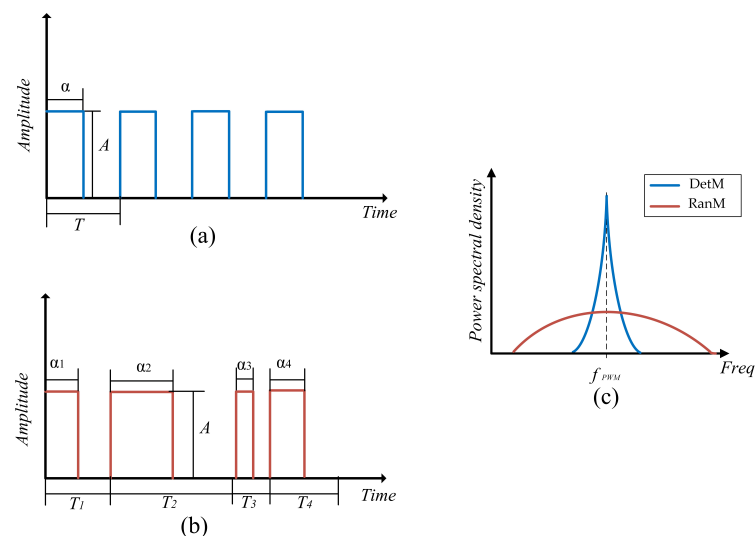


Figure 1. The schematic view of signals (a) DetM in time domain, (b) RanM in time domain, and (c) both modulations in frequency domain.

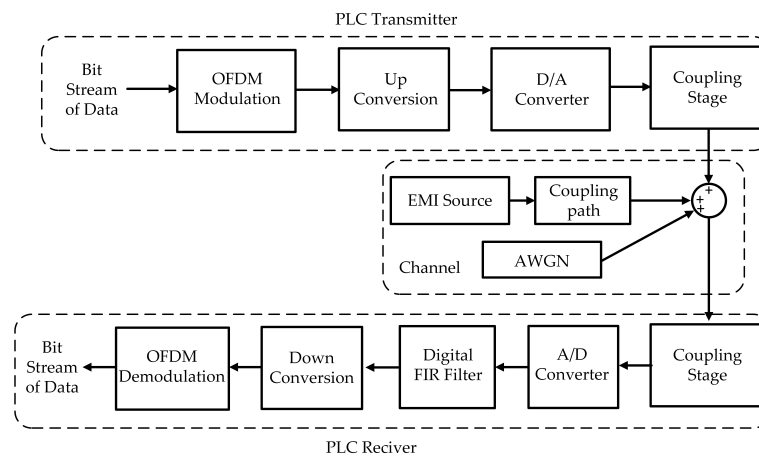
3. Description of the G3-PLC Operation

In this research we focus on using the G3-PLC technology, which follows the European Norm (EN) 50065 that CENELEC established in 1992 [7]. The PLC works by modulating the carrier signal using M-ary Phase Shift Keying (M-PSK), which is a type of digital modulation scheme. Usually, the G3-PLC systems use one of three types of PSK: Binary PSK (BPSK), Quad PSK (QPSK), and 8-PSK. The differences are due to the number of simultaneously coded states. The G3-PLC use the differential PSK (DPSK) in which input information modulates the phase change, not the absolute value of the phase. After that, the data are distributed through multi-carrier frequencies using orthogonal frequency division multiplexing (OFDM) with the following physical layer (PHY) specifications shown in Table 1 [26].

Table 1. G3-PLC specifications.

Specification	G3-PLC
Frequency Range	35–91 kHz
Sampling Frequency f_s	400 kHz
FFT size	256
Length of Cyclic Prefix	30
Sub Carrier Spacing	1.5625 kHz
No. of Carriers Used	36
Max data Rate	33.4 kbps
Modulation	DBPSK, DQPSK, and D8PSK

Figure 2 shows the block diagram of the G3-PLC PHY layer. We can divide the PHY layer of the G3-PLC system into three main elements:

**Figure 2.** The PHY layer of the G3-PLC system.

3.1. PLC Transmitter

The process of sending the data starts by getting digital information to be transmitted using the OFDM modulation technology. The result is a list of the amplitudes and phases that are distributed through a definite range of frequencies. After that, the digital up-converter takes the digital signal from the OFDM and is multiplied by a carrier frequency [26]. The transmitted signal is quantized using the digital-to-analog converter (D/A) inside the controller with a specific quantized step size according to the size of the D/A [27].

3.2. PLC Receiver

Demodulation of the received signal starts with passing the carrier signal through a coupling circuit to extract the PLC signal from the main grid power (220 V–50 Hz). After that, the analog signal is converted into a digital signal using an analog-to-digital (A/D) converter. Furthermore, a digital finite impulsive response (FIR) filter is used, followed by a digital down converter to extract the digital data from the carrier signal. Consequently, the data are demodulated and demapped to return to its digital binary form.

3.3. Channel

The PLC transmission channel practically represents power cables. The signal attenuates with the length of the line according to the properties of copper wires and their insulation. In the channel, the conducted electromagnetic disturbances interfere with the PLC signal through a coupling path, in addition to the additive white Gaussian noise (AWGN). The channel models are usually represented by their channel response function $H(f)$. Based on [11], the channel could be a flat channel, frequency selective channel,

or phase shift channel, according to the way that the FIR filter in the receiver recognizes it. This paper considers the coupling between the EMI disturbance and the G3-PLC through the mutual coupling between cables as introduced in the next section.

4. Proposed Experimental Setup

The proposed hardware setup is inspired by the EMI between power electronics converter and a smart meter utilizing the G3-PLC. Such a case is typical in the microgrid environment, where renewable energy sources are installed in the same place as the smart meter. The EMI may flow between both circuits due to the mutual coupling between circuit cables. The communication circuit consists of two G3-PLC modems representing the point-to-point communication between a specific transmitter and receiver. The circuit works using two Microchip ATPL360 PLC modems as shown in Figure 3, with both modems being configured to work based on CENELEC-A standard frequency range and the G3-PLC mode. In addition, the line stabilization impedance network (LISN) and isolation transformer are connected between the PLC circuit and the grid to isolate the outside EMI noise and make sure of the robustness of the results.

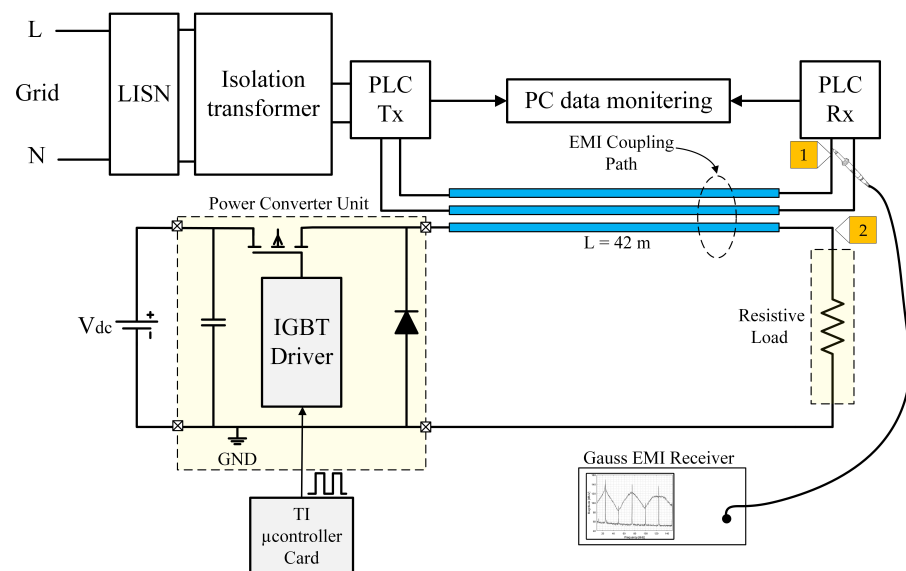
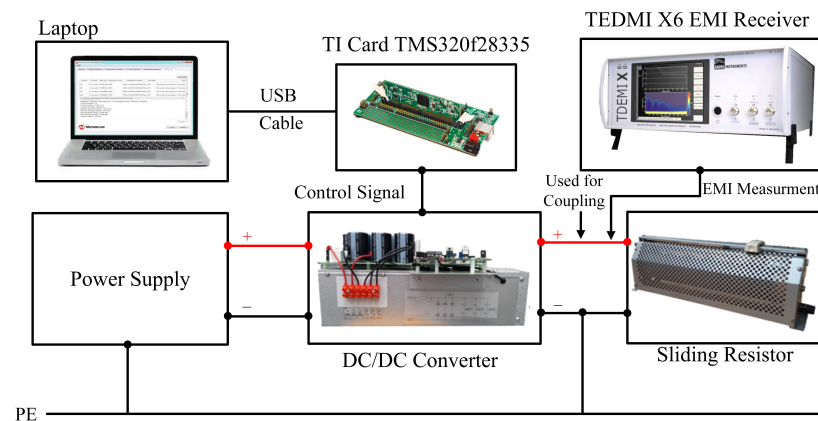


Figure 3. Connection diagram of the proposed experimental setup.

The EMI source is represented in the power connection between a DC/DC converter and the load. The load is connected to the converter using a cable of 42 m length, and the positive line of the load is situated directly beside the PLC cables with the length as shown in Figure 3. The cable in the tests is a typical YDyp AKS $3 \times 1.5 \text{ mm}^2$ cable used in domestic installations. This connection is similar to the link in [14] and will cause the existence of coupling between both circuits. The DC/DC converter was controlled using a Texas Instrument TMS320F28335 digital signal processing card and was connected to a variable DC supply changing from 100 V to 200 V. Table 2 shows the electrical data for the converter used in the setup. The DC/DC step-down converter topology was selected as an interference source due to its simple waveform of generated interference, which might be easily investigated. In the same context, the RanM driving signal parameters play an important role in the shape of the generated EMI. The spreading factor of the used RanM is set at 0.4, which means that based on Equation (1), the frequency will vary around the main switching frequency between $0.8 f_{PWM}$ kHz to $1.2 f_{PWM}$ kHz. Figure 4 shows the connection diagram of the proposed DC power circuit. In our implementation of the test in the laboratory, we used a sliding resistor as the load. For both communication and power circuits, we used copper cables of diameter 1.5 mm^2 .

Table 2. DC/DC converter electrical data.

Item	Value/Type
Transistor type	IXGH40N60C2D1
Input Voltage	From 100 V to 200 V
Output Voltage	From 50 V to 100 V
Load current	From 0.83 A to 1.667 A
Switching main frequency	Varies from 50 kHz to 75 kHz
Duty cycle	0.5

**Figure 4.** Connection diagram of the DC/DC converter control.

5. Experimental Results and Discussion

The Gauss Instruments TDMI X6 digital EMI test receiver was used to register the measurements. All the measurements were taken based on CISPR A standard in the range from 9 kHz to 150 kHz, using the Average (AV) and quasi-peak (QP) detectors with 200 Hz intermediate frequency bandwidth (IF BW).

5.1. PLC Configuration and Measurements

Table 3 shows the PLC communication parameter assumptions. The test was implemented using 3000 packets that were sent consequently. The time between packets was 100 ms, the modulation scheme used was the differential phase shift keying (DPSK) with all three types (DBPSK, DQPSK, and D8PSK). As the G3-PLC uses the CENELEC-A standard, the frequency range of the PLC OFDM signal is in the frequency range between 35 and 91 kHz, as shown in the QP and AV detectors frequency spectrum in Figure 5 (measured from point 1 in Figure 3). The level of the PLC spectrum reaches 85 dBuV for the AV detector at the intermediate frequency (63 kHz) of the PLC signal. The streaming of the PLC data in the time domain appears in the PLC voltage after the bandpass filter in the receiver as shown in Figure 6.

Table 3. PLC communication assumptions.

Item	Value/Type
Type of PLC communication standard	G3-PLC
Data size	65 bytes
Physical Layer	OFDM
Modulation	DBPSK-DQPSK-D8PSK
Total sent Frames	3000
The time between each packet	100 ms
The Medium	Single-phase cable of Length 42 m

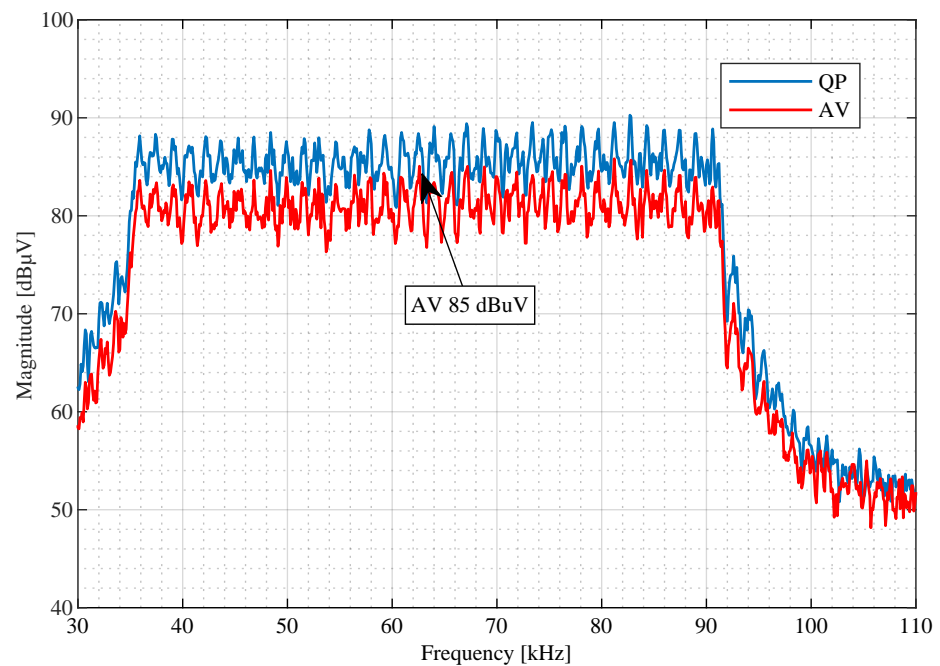


Figure 5. The spectrum of G3-PLC signal.

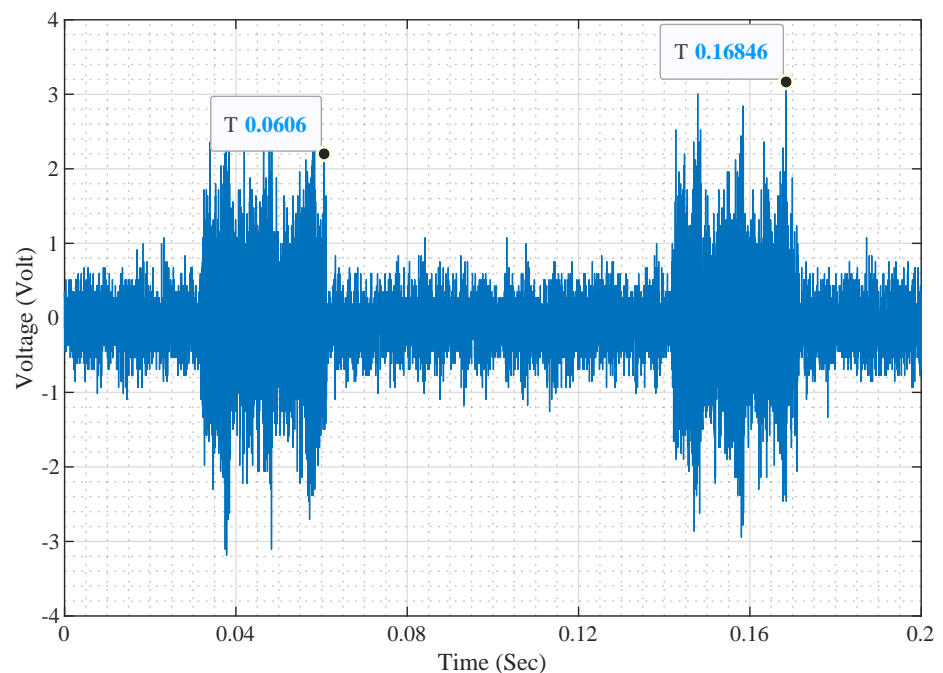


Figure 6. G3-PLC signal in the time domain.

5.2. Deterministic and Random Configuration and Measurements

In this paper we consider two operating scenarios, one is the change in the amplitude of the noise, the other is the change in the converter main switching frequency.

5.2.1. The Variation in the EMI Amplitude

The converters were programmed to work using a switching frequency of 63 kHz, equal to the intermediate frequency of the PLC OFDM signal. The selected frequency is within the typical operating frequency range of medium power converters. Figure 7 shows

the voltage spectrum measured directly from the load terminals in the case of DetM and RanM at 50 V and 100 V DC output voltages using the AV detector (measured from point 2 in Figure 3). As shown in the figure, the difference between the output voltage spectrum in the DetM and RanM at the fundamental frequency reaches almost 17 dB. The impact of the DC/DC converter output has its effect on the PLC circuit through the proposed coupling circuit as shown in Figure 8. The figure shows the frequency spectrum of DetM and RanM in the case of an output voltage of 50 V and 100 V measured from the PLC side (from point 1 in Figure 3) using an AV detector. The maximum magnitude of the spectrum (at the main switching frequency of the converter 63 kHz) reaches 81.6 dBuV for DetM and 63 dBuV for RanM at 50 V output voltage, and it reaches 87.5 dBuV and 69 dBuV in case of 100 V. It was noticed that the difference between both output voltages is 6 dB in both cases of modulations at the main converter switching frequency. The difference between RanM and DetM also reaches 18.8 dB at the same point. The achieved disturbance levels in the network are close to the limit levels, according to CISPR 11.

Figure 9 shows the percentage of data transmission error with the increase in the DC/DC converter output voltage ranging from 50 V to 100 V for the converter circuit in the case of DetM and RanM, along with the change in the PLC modulation. The ratio between the corrupted frames data to the sent data is calculated for every case to be the frame error rate (FER) and is represented as a percentage and can be formulated as

$$FER = \frac{Broken\ Frames}{Sent\ Frames} \times 100. \quad (3)$$

The results show that data transmission FER increases with the increasing noise signal magnitude. Moreover, both techniques have almost the same effect on the data transmission streaming in all PLC modulation cases (DBPSK, DQOSK, and D8PSK). The difference between the DetM and RanM increases with the increase of the voltage magnitude, and the maximum difference reaches 5%. Table 4 shows the probability of G3-PLC data transmission FER, with the increase in output voltage for both modulations and various PLC modulation techniques.

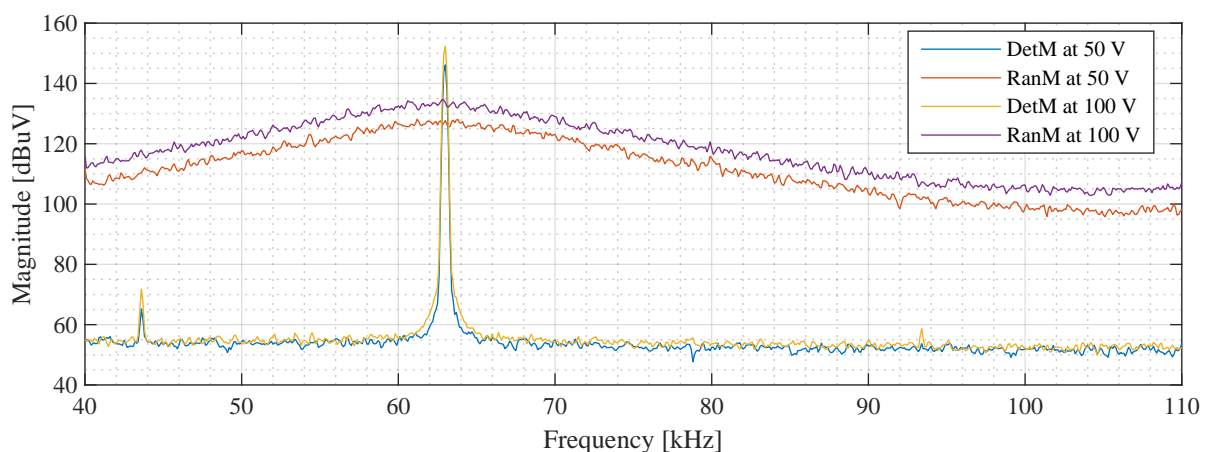


Figure 7. The frequency spectrum of DC/DC converter output at point 2 for DetM and RanM.

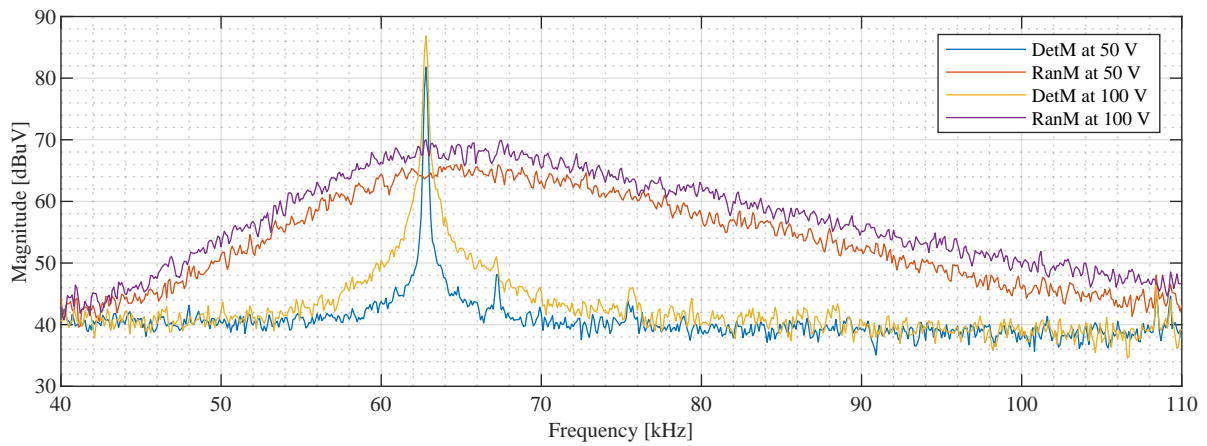


Figure 8. The frequency spectrum of DC/DC converter measured at grid terminal (point 1) for DetM and RanM.

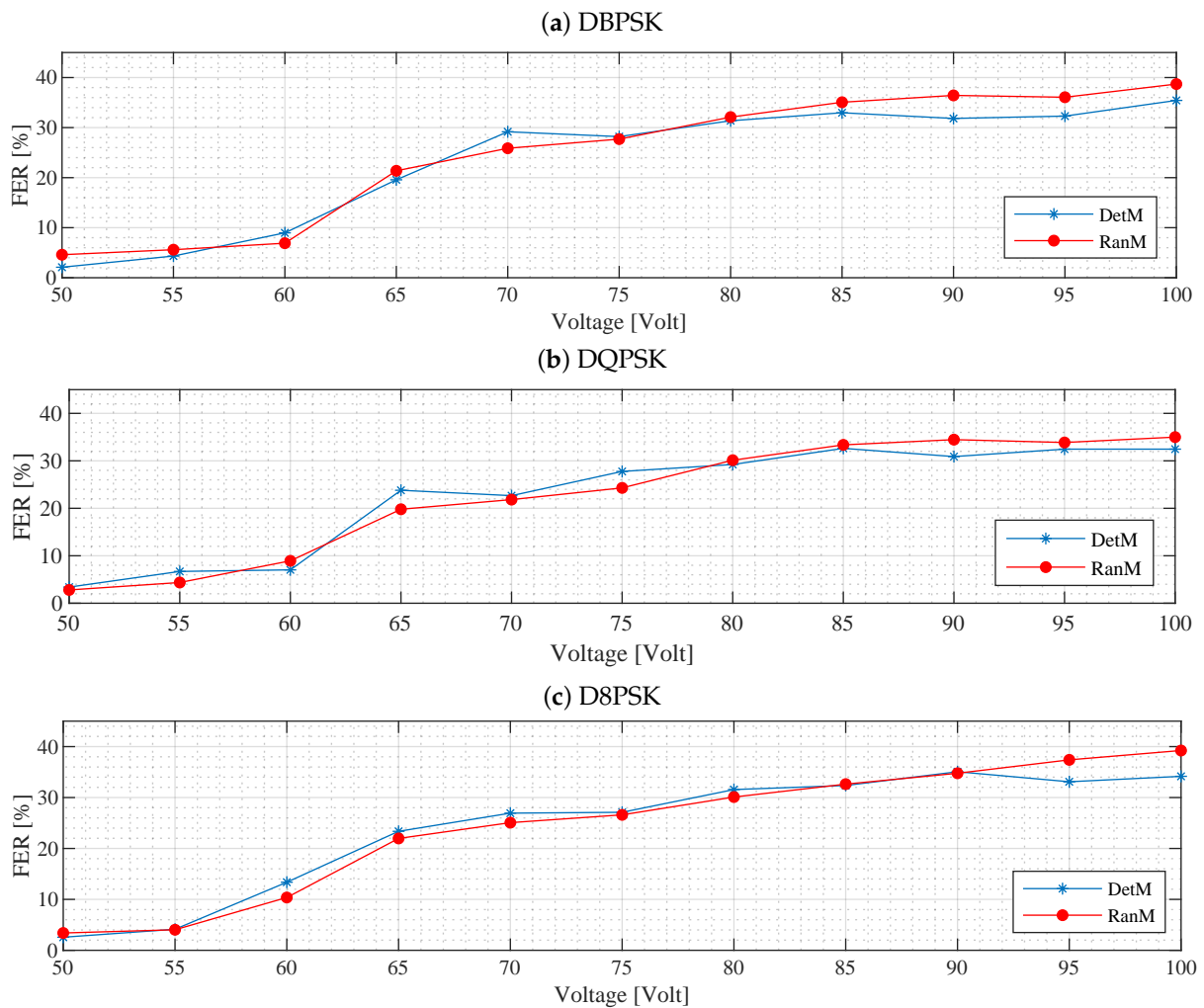
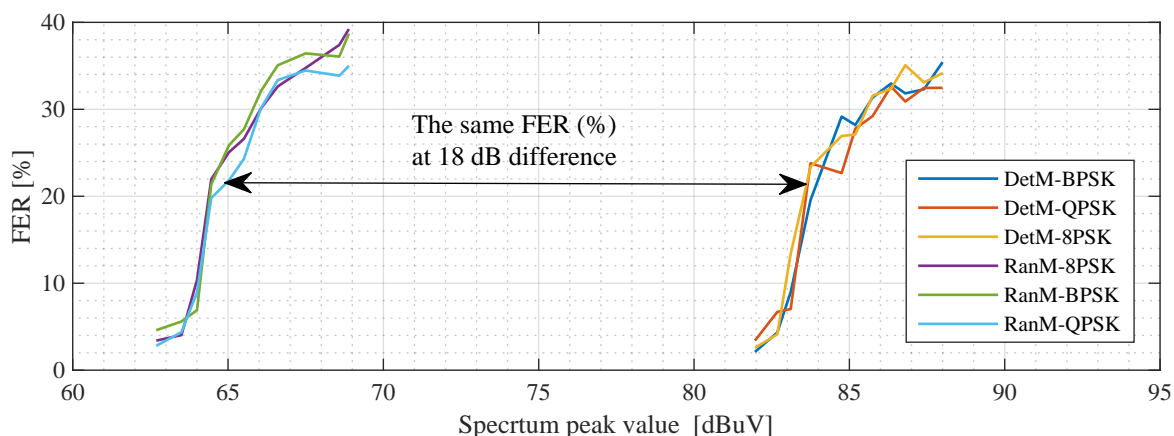


Figure 9. The percentage FER for different output voltages and PLC modulation schemes in the case of using different converter modulations for DBPSK (a), DQPSK (b), D8PSK (c).

Table 4. The probability of data transmission error in the PLC with the increase in supply voltage.

FER (%) in the Case of DetM					FER (%) in the Case of RanM			
Volt	dBuV	DBPSK	DQPSK	D8PSK	dBuV	DBPSK	DQPSK	D8PSK
50	81.80	2.10	3.40	4.13	63.00	4.60	2.80	4.33
75	85.00	28.2	27.76	27.10	65.51	27.70	24.36	26.60
100	87.00	35.43	32.46	34.16	69.00	38.07	35.00	39.23

Figure 10 shows the relation between the frequency spectrum peak (measured from point 1 in Figure 3). In both modulation cases, the increase in the magnitude of the noise is followed by an increase in the percentage of FER, respectively. However, the FER is almost the same, despite an 18 dB difference in the spectrum peak value. Figure 11 shows the relation between the output voltage from the converter and the frequency spectrum magnitude in dBuV (measured from point 1 in Figure 3). In both DetM and RanM, the EMI receiver IFBW is set to 200 Hz following CISPR A standard, and the relation is linear in both cases. However, the difference between the frequency spectrum magnitude reaches almost 18 dB between the DetM and RanM. Figure 12 shows the same result as in Figure 11, but with different IFBW configurations in the EMI receiver set at 9 kHz, the difference between the DetM and RanM is on average of 3.5 dBuV at all voltage points, which confirms the symmetry of both techniques. Consequently, a difference appears between both techniques resulting from the methodology of the EMI spectrum measurement.

**Figure 10.** FER Vs Magnitude in dBuV for different PLC modulation schemes in case of DetM and RanM.

5.2.2. The Variation in the Converter Main Switching Frequency at Constant EMI Noise

Figure 13 shows the FER results in the case of varying the converter main switching frequency around the intermediate value of the G3-PLC bandwidth from 50 kHz to 75 kHz, at a constant converter output voltage of 75 V. The G3-PLC modem is configured to work using the BPSK. The results show that both techniques have the same effect on the G3-PLC performance at the main switching frequency equal to the intermediate frequency of the G3-PLC (63 kHz).

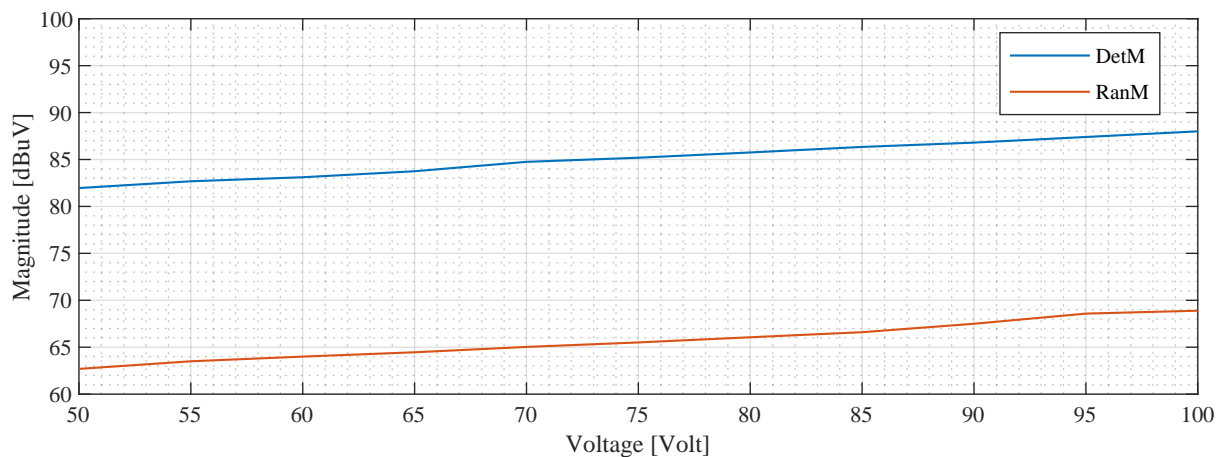


Figure 11. The maximum amplitude of disturbances, measured at the grid terminal (point 1, Figure 3) depending on the converter supply voltage for different modulation schemes (DetM and Ran) for IFBW = 200 Hz.

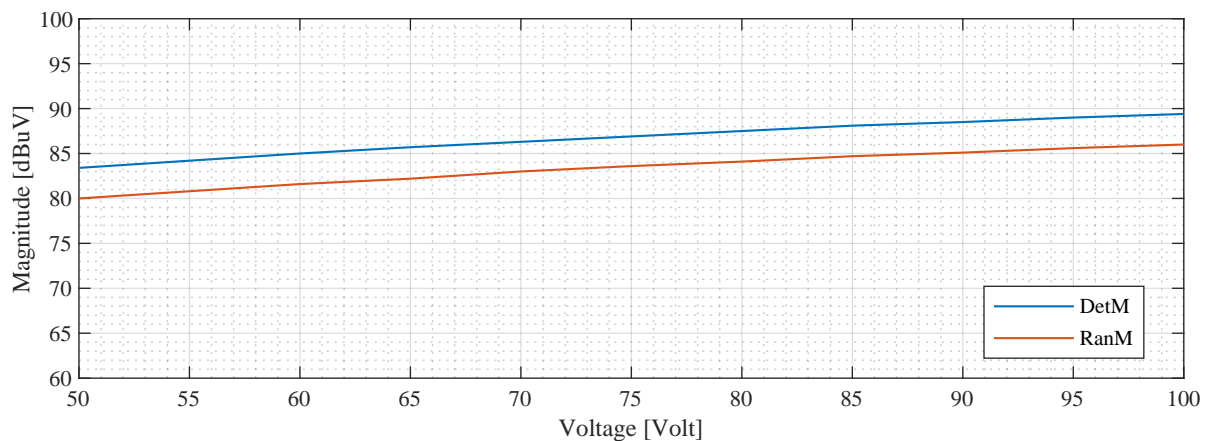


Figure 12. The maximum amplitude of disturbances, measured at the grid terminal (point 1, Figure 3) depending on the converter supply voltage for different modulation schemes (DetM and Ran) for IFBW = 9 kHz.

In contrast, on the other frequencies near to the intermediate frequency, the RanM causes more problems to the PLC systems than in the DetM. The randomized signal increases the percentage of FER in the case of other frequencies due to the fast jumping between the frequencies around the main switching frequency (central frequency f_{PWM}). On the other hand, the DetM affects only specific points in the PLC bandwidth, which could be a sensitive point in the communication system as in the case of choosing a switching frequency equal to the intermediate frequency of the G3-PLC system.

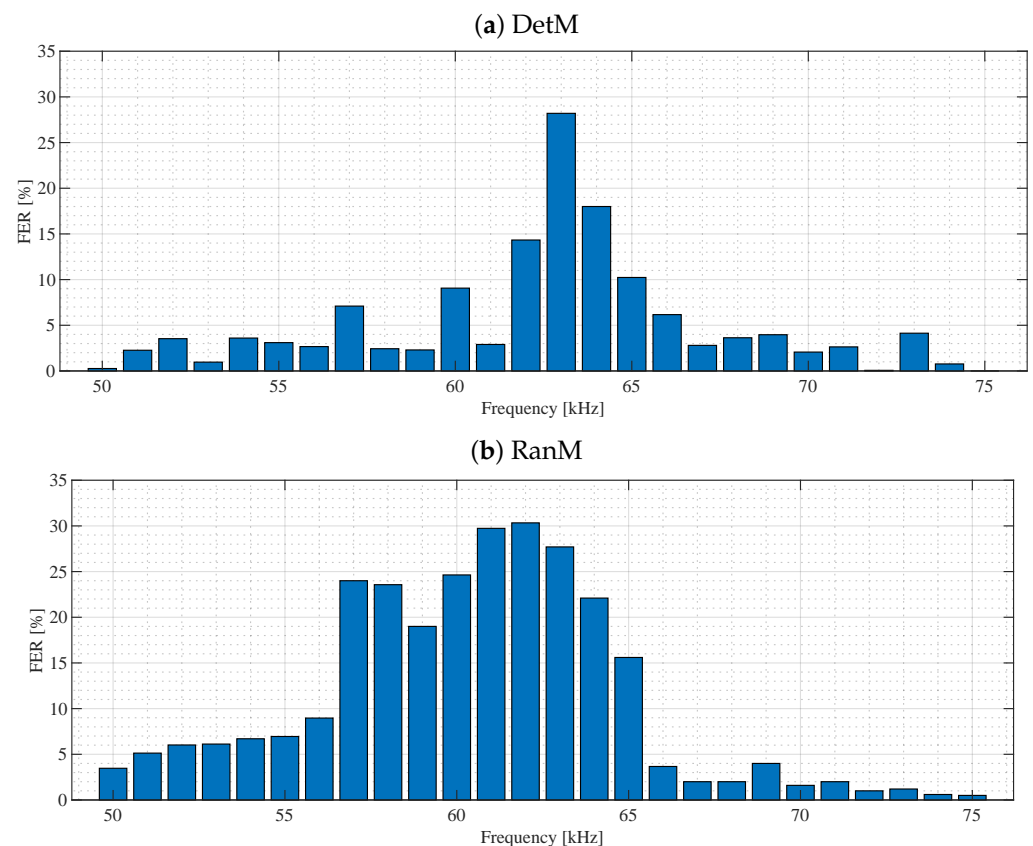


Figure 13. The FER percentage vs. the variation in the main switching frequency values around the intermediate frequency of the G3-PLC bandwidth for DetM (a) and RanM (b).

6. Conclusions

The results presented in the paper focused on the impact of the DC/DC step-down converter, treated as a source of EMI noise, on the narrowband G3-PLC. The hardware setup was designed to provide an opportunity for comparative investigations between DetM and RanM converter modulation strategies. Furthermore, the designed hardware configuration allowed variable DC supply (interference level) and selection of different PLC phase-shift keying modulation and the converter main switching frequency. All the measurements were taken in the CISPR A frequency range (9 kHz to 150 kHz) using the quasi-peak and average detectors. Particular advantages of RanM resulting from lowering the level of the EMI spectrum measured according to currently binding regulations may help meet the EMI limits set by EMC standards. However, the experimental results of transmission errors have indicated that in the analyzed frequency range, there is no significant difference between the effect of DetM and RanM, despite the considerable decrease in spectrum magnitude by RanM (which sometimes reaches 20 dB—ten times). The obtained results show a relationship between the data transmission error and the level of converter voltage, which is linked with the disturbance energy. The influence of both modulations was also studied in the case of various switching frequencies. The results showed that the RanM might deliver even more problems connected with PLC transmission reliability than the DetM. Similar results were already known in the literature for simple encrypted communication standards such as RS-232 or I2C. In the article, we confirmed these conclusions for PLC communication systems that use advanced data encoding methods and input selectivity.

We can also assume that the spectrum of disturbances measured by the receiver cannot be taken as a factor for assessing the quality of the PLC communication channel. Spectrum measurement with an EMI receiver is sensitive to the nature of the measured signals. The change of the IFBW in measurement equipment for RanM significantly changes the measured values of the disturbance spectrum (Figures 12 and 13). During the

measurement, disturbances in the entire communication channel should be aggregated to be adequately assessed. Additionally, the robustness of various data encoding techniques in PLC communication has been tested. The data transmission error is almost the same for different DPSK modulation techniques (BPSK, QPSK, and 8PSK) applied in PLC devices. The observed FER values for the PLC-sent data in all the investigated DPSK modulations are practically the same. The results may be surprising as the data from the literature have shown significant differences in the immunity of different DPSK coding methods to disturbances. The reason is that converters' real signals are more complicated than typical test signals (white noise, harmonic signal, and periodic pulse signal).

Author Contributions: Conceptualization, W.E.S., P.L., R.S., A.M., M.P., and A.K.; methodology, W.E.S., P.L., and R.S.; software, W.E.S. and A.M.; validation, W.E.S. and P.L.; investigation, W.E.S., P.L., and R.S.; resources, R.S., P.L., and A.K.; writing—original draft preparation, W.E.S. and P.L.; writing—review and editing, W.E.S., P.L., R.S., A.M., M.P., and A.K.; supervision, R.S. and P.L.; project administration, R.S.; funding acquisition, R.S. All authors have read and agreed to the published version of the manuscript.

Funding: This paper is part of two projects that have received funding from the European Union's Horizon 2020 research and innovation program under the Marie Skłodowska-Curie grant agreements No 812391-SCENT and No 812753-ETOPIA.

Conflicts of Interest: The authors declare no conflict of interest.

References

1. Roggo, D.; Horta, R.; Capponi, L.; Eggenschwiler, L.; Decorvet, F.; Pellodi, C.; Buholzer, F. Electromagnetic interferences in smart grid applications: A case study with power line communication smart meters and PV energy generation. *CIREC Open Access Proc. J.* **2017**, *2017*, 607–611. [\[CrossRef\]](#)
2. Kilani, K.; Degardin, V.; Laly, P.; Lienard, M.; Degauque, P. Impulsive noise generated by a pulse width modulation inverter: Modeling and impact on powerline communication. In Proceedings of the 2013 IEEE 17th International Symposium on Power Line Communications and Its Applications, Johannesburg, South Africa, 24–27 March 2013; pp. 75–79.
3. Limas, M.; Agudelo-Martinez, D.; Rodríguez, J.B.; Pavas, A. Conducted emission variations using low power LED lamps connected to other devices. In Proceedings of the 2018 18th International Conference on Harmonics and Quality of Power (ICHQP), Ljubljana, Slovenia, 13–16 May 2018; pp. 1–6. [\[CrossRef\]](#)
4. Jettanasen, C.; Ngaopitakkul, A. The Conducted Emission Attenuation of Micro-Inverters for Nanogrid Systems. *Sustainability* **2020**, *12*, 151. [\[CrossRef\]](#)
5. Kotsampopoulos, P.; Rigas, A.; Kirchhof, J.; Messinis, G.; Dimeas, A.; Hatziargyriou, N.; Andreadis, K. EMC Issues in the Interaction Between Smart Meters and Power-Electronic Interfaces. *IEEE Trans. Power Deliv.* **2017**, *32*, 822–831. [\[CrossRef\]](#)
6. Rönnerberg, S.K.; Bollen, M.H.; Amaris, H.; Chang, G.W.; Gu, I.Y.; Kocewiak, Ł.H.; Desmet, J. On waveform distortion in the frequency range of 2 kHz–150 kHz—Review and research challenges. *Electr. Power Syst. Res.* **2017**, *150*, 1–10. [\[CrossRef\]](#)
7. Cano, C.; Pittolo, A.; Malone, D.; Lampe, L.; Tonello, A.M.; Dabak, A.G. State-of-the-art in Power Line Communications: From the Applications to the Medium. *IEEE J. Sel. Areas Commun.* **2016**, *8716*, 1–19. [\[CrossRef\]](#)
8. Meyer, J.; Khokhlov, V.; Klatt, M.; Blum, J.; Waniek, C.; Wohlfahrt, T.; Myrzi, J. Overview and Classification of Interferences in the Frequency Range 2–150 kHz (Supraharmonics). In Proceedings of the SPEEDAM 2018—Proceedings: International Symposium on Power Electronics, Electrical Drives, Automation and Motion, Amalfi, Italy, 20–22 June 2018; pp. 165–170.
9. Korki, M.; Hosseinzadeh, N.; Moazzeni, T. Performance evaluation of a narrowband power line communication for smart grid with noise reduction technique. *IEEE Trans. Consum. Electron.* **2011**, *57*, 1598–1606. [\[CrossRef\]](#)
10. Di Bert, L.; Caldera, P.; Schwingshackl, D.; Tonello, A.M. On Noise Modeling for Power Line Communications. In Proceedings of the 2011 IEEE International Symposium on Power Line Communications and Its Applications, Udine, Italy, 3–6 April 2011; pp. 283–288.
11. Llano, A.; Angulo, I.; Angueira, P.; Arzuaga, T.; De la Vega, D. Analysis of the Channel Influence to Power Line Communications Based on ITU-T G.9904 (PRIME). *Energies* **2016**, *9*, 39. [\[CrossRef\]](#)
12. Bojarski, J.; Smolenski, R.; Kempinski, A.; Lezynski, P. Pearson's random walk approach to evaluating interference generated by a group of converters. *Appl. Math. Comput.* **2013**, *219*, 6437–6444. [\[CrossRef\]](#)
13. Bojarski, J.; Smolenski, R.; Lezynski, P.; Sadowski, Z. Diophantine equation based model of data transmission errors caused by interference generated by DC-DC converters with deterministic modulation. *Bull. Pol. Acad. Sci. Tech. Sci.* **2016**, *64*, 575–580. [\[CrossRef\]](#)
14. Li, K.J.; Xie, Y.Z.; Zhang, F.; Chen, Y.H. Statistical Inference of Serial Communication Errors Caused by Repetitive Electromagnetic Disturbances. *IEEE Trans. Electromagn. Compat.* **2019**, *62*, 1160–1168. [\[CrossRef\]](#)

15. Chen, H.; Wang, T. Estimation of Common-Mode Current Coupled to the Communication Cable in a Motor Drive System. *IEEE Trans. Electromagn. Compat.* **2018**, *60*, 1777–1785. [[CrossRef](#)]
16. Adrian, V.; Chang, J.S.; Gwee, B.H.; Tedjaseputro, S. Spectral Analysis of Randomized Switching Frequency Modulation Scheme with a Triangular Distribution for DC-DC Converters. In Proceedings of the 2009 International Conference on Computing, Engineering and Information, Fullerton, CA, USA, 2–4 April 2009; pp. 119–122.
17. Cui, K.; Adrian, V.; Sun, Y.; Gwee, B.H.; Chang, J.S. A Low-Harmonics Low-Noise Randomized Modulation Scheme for Multi-Phase DC-DC Converters. In Proceedings of the 15th IEEE International New Circuits and Systems Conference (NEWCAS), Strasbourg, France, 25–28 June 2017; pp. 165–168.
18. Pareschi, F.; Rovatti, R.; Setti, G. EMI Reduction via Spread Spectrum in DC/DC Converters: State of the Art, Optimization, and Tradeoffs. *IEEE Access* **2016**, *3*, 2857–2874. [[CrossRef](#)]
19. CENELEC-EN 55011:2016. *Industrial, Scientific and Medical Equipment—Radio-Frequency Disturbance Characteristics—Limits and Methods of Measurement*; CEN-CENELEC: Brussels, Belgium, 2016.
20. Crovetto, P.S.; Musolino, F. Interference of Spread-Spectrum EMI and Digital Data Links under Narrowband Resonant Coupling. *Electronics* **2020**, *9*, 60. [[CrossRef](#)]
21. Musolino, F.; Crovetto, P.S. Interference of Spread-Spectrum Switching-Mode Power Converters and Low-Frequency Digital Lines. In Proceedings of the 2018 IEEE International Symposium on Circuits and Systems (ISCAS), Florence, Italy, 27–30 May 2018; p. 5.
22. Lezynski, P.; Smolenski, R.; Loschi, H.; Thomas, D.; Moonen, N. A novel method for EMI evaluation in random modulated power electronic converters. *Measurement* **2020**, *151*, 107098. [[CrossRef](#)]
23. Lezynski, P. Random Modulation in Inverters With Respect to Electromagnetic Compatibility and Power Quality. *IEEE J. Emerg. Sel. Top. Power Electron.* **2018**, *6*, 782–790. [[CrossRef](#)]
24. Lai, Y.; Member, S.; Chang, Y. Novel Random-Switching PWM Technique With Constant Sampling Frequency and Constant Inductor Average Current for Digitally Controlled Converter. *IEEE Trans. Ind. Electron.* **2013**, *60*, 3126–3135. [[CrossRef](#)]
25. Mathe, L.; Lungeanu, F.; Sera, D.; Rasmussen, P.O.; Pedersen, J.K. Spread Spectrum Modulation by Using Asymmetric-Carrier Random PWM. *IEEE Trans. Ind. Electron.* **2012**, *59*, 3710–3718. [[CrossRef](#)]
26. Matanza, J.; Alexandres, S.; Rodriguez-Morcillo, C. Performance evaluation of two narrowband PLC systems: PRIME and G3. *Comput. Stand. Interfaces* **2013**, *36*, 198–208. [[CrossRef](#)]
27. Schwarz, M.; Gronwald, F. EMI analysis of a generic power line communication OFDM data link. In Proceedings of the EMC Europe 2011 York—10th International Symposium on Electromagnetic Compatibility, York, UK, 26–30 September 2011; pp. 625–628.